Journal of Thermal Analysis and Calorimetry, Vol. 72 (2003) 25–33

TRANSFORMATION DIAGRAMS
Isoconversional method from calorimetric data

J. J. Suñol[*]

Grup de Recerca en Materials i Termodinàmica, Universitat de Girona, E-17071 Girona, Spain

Abstract

Transformation diagrams are one of the most reliable ways to predict the thermal behavior of the materials. In this work, the crystallization process of several metallic glasses and polymer materials was analyzed and two isoconversional methods are applied to perform kinetic analysis of non-isothermal heating/cooling and isothermal processes.

Moreover, the diagrams were constructed from modeling experimental data without the knowledge of the kinetic model. There was a good agreement between experimental data and the calculated curves, which verifies the reliability of the method and the validity of the rate constant model description.

Keywords: DSC, isoconversional methods, transformation diagrams

Introduction

The knowledge of the thermodynamic behavior of materials, i.e. the crystallization transformation diagrams, is important to control their structure and modify their properties. For instance, processes as crystallization promote changes in materials properties. In the modeling of the crystallization process, we will distinguish cold crystallization as against solidification from the melt. Both crystallization processes will be produced under isothermal or dynamic (heating or cooling) regime. The main difference is that cold crystallization of a material may be promoted by pre-existing nuclei. However, solidification from the melt it is expected to be driven by nucleation [1].

The classical theories of nucleation and crystal growth have been developed independently by several authors [2–4]. Transformation diagrams are one of the most reliable ways to predict the thermal behavior of the material. They have led to the determination of time–temperature–transformation, T–T–T, curves for the description of the isothermal crystallization reaction since the work of Uhlmann [5]. The recent literature demonstrates that this field presents a great scientific interest. The T–T–T diagrams are widely applied to study the kinetic of solid state reactions and solidification; i.e., the thermal stability of glasses [6], the eutectic decomposition in solidified

---

[*] Author for correspondence: E-mail: joanjosep.sunyol@udg.es

1388–6150/2003/ $ 20.00

Akadémiai Kiadó, Budapest
Kluwer Academic Publishers, Dordrecht

alloys [7], the cure behavior of resins [8], the liquid crystalline phase and time to gelation [9] or the solid state transformations in metallic alloys [10]. Experimentally, the crystallization kinetics of materials can be assessed by numerous conventional techniques as X-ray diffraction complemented with microstructure observation [11], resistivity measurements [10], transmission electron microscopy (TEM) [12] or scanning probe microscopy (SPM) [13]. In particular, the thermoanalytical techniques (TA), such as differential thermal analysis (DTA), and differential scanning calorimetry (DSC) are ones of the most often applied [14–15].

Furthermore, two transformation diagrams have been introduced [16–17] to describe non-equilibrium crystallization under continuous heating or cooling regimes, namely the T–HR–T (temperature–heating rate–transformation) and T–CR–T (temperature–cooling rate–transformation) diagrams. In this work the crystallization process, cold crystallization process and solidification from the melt, are analyzed using two isoconversional methods to obtain the transformation diagrams: temperature–heating/cooling rate and temperature–time. The thermal study is performed by means of differential scanning calorimetry (DSC). All transformation curves are obtained from the analysis of non-isothermal calorimetric experiments in several materials: Fe–Ni based metallic glasses obtained by rapid solidification and polymer blends with PEG6000 (PEG–PD).

Crystallization kinetics

Cold crystallization

To explain the thermal behavior on crystallization, each crystallization step is assumed to have a rate of transformation given by the direct derivative of the well-known JMAE expression [2–4, 18]

$$\frac{\mathrm{d}\alpha}{\mathrm{d}t}=K(T)f(\alpha) \tag{1}$$

with $K(T)$ the rate constant which presents a different form under homogeneous nucleation and for growth of preexisting nuclei and with $f(\alpha)$ a function describing the mechanism governing the crystallization process. The rate constant is a function of the nucleation frequency and the crystal growth rate. Very often these values are not experimentally known, and then the rate constant is arbitrarily assumed to be given by the following Arrhenius expression in the cold crystallization.

$$K(T)=k_0\exp(-E/RT) \tag{2}$$

where the pre-exponential factor, k_0, and the apparent activation energy, E, can be deduced from calorimetric measurements, both quantities assumed to be practically independent of temperature in the temperature interval analyzed.

Several methods can be applied to obtain the activation energy. Kinetic analysis of the non-isothermal data has been subject of numerous criticisms [19–21]. In the case of a complex mechanism, peak area evolution methods and model-fitting methods give only a mean value of the kinetic parameters and isoconversional methods can be used to elucidate the kinetics of the process [19]. In our work, the isoconversional method developed by Málek [22–24] is applied to obtain the *E* value from non-isothermal DSC scans at several heating rates in the crystallization process of Fe–Ni based alloys produced by rapid solidification.

Under isothermal conditions, Eq. (1) can be integrated to give

$$g(\alpha)=\int_0^{\alpha'}\frac{1}{f(\alpha)}\mathrm{d}\alpha=k_0\exp\left(-\frac{E}{RT}\right)t \tag{3}$$

This equation, when represented as temperature *vs.* the time needed for crystallization of a fixed fraction, α, of the material, gives the T–T–T curve.

By the same procedure, integration of Eq. (1) under constant rate temperature variation, β, gives

$$g(\alpha)=\int_0^{\alpha'}\frac{1}{f(\alpha)}\mathrm{d}\alpha=\frac{k_0}{\beta}\int\exp\left(-\frac{E}{RT}\right)\mathrm{d}T \tag{4}$$

The solution obtained can be represented in a T–HR–T diagram. Usually, the values for the crystallization process that are obtainable from DSC experiments [25] and which are essential in the empirical determination of the low-temperature parts of the T–T–T and T–HR–T curves are the activation energy and $k_0f(\alpha)$.

Once the value of *E* is known, it is usual to evaluate the function $f(\alpha)$ from the continuous heating experiments and to compare the value obtained with that obtained in the isothermal experiments [26]. However, a method of obtaining T–HR–T and T–T–T diagrams from non-isothermal data assuming the same crystallization process under isothermal conditions can be applied. T–HR–T curves can be obtained by integration from Eq. (1) under continuous heating rate [6]

$$\beta=\frac{k_0RT^2\exp(-E/RT)}{E\int_0^{\alpha}\frac{\mathrm{d}\alpha}{f(\alpha)}} \tag{5}$$

and T–T–T curves can be obtained by integration from Eq. (1) under isothermal conditions

$$t=\exp(-E/RT)\int_0^{\alpha}\frac{\mathrm{d}\alpha}{f(\alpha)} \tag{6}$$

By using the following equation, one can solve the integral of previous equations even if the value of $f(\alpha)$ is unknown:

$$\int_0^{\alpha}\frac{\mathrm{d}\alpha}{k_0f(\alpha)}=\int_0^{\mathrm{T}}\frac{\exp(-E/RT)}{\beta}\mathrm{d}T \tag{7}$$

To calculate T–HR–T and T–T–T diagrams, it is necessary to solve the right integral of previous equation; the only experimental data is the activation energy of the process. This approach is applied to the study of the crystallization behavior of several Fe–Ni based metallic glasses obtained by rapid solidification, Figs 1 and 2 show the T–HR–T curves calculated with the experimental data that correspond to α values of 0.1, 0.5 and 0.9. Curves were compared with the experimental data from measurements at other heating rates to check the methodological validity. The results correlated well, which verifies the reliability of the method utilized. Figure 3 shows the T–T–T diagram. In a very similar way to the T–HR–T case, the curves obtained were compared with experimental isothermal data. The major application of the T–HR–T (T–T–T) curves is for prediction of the amount

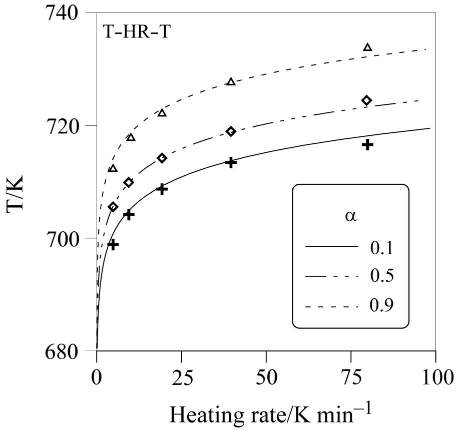

Fig. 1 Temperature–Heating Rate–Transformation diagram of the crystallization process of an Fe–Ni based metallic glass. Experimental data (symbols) and calculated curves (lines) for transformed fractions 0.1, 0.5 and 0.9

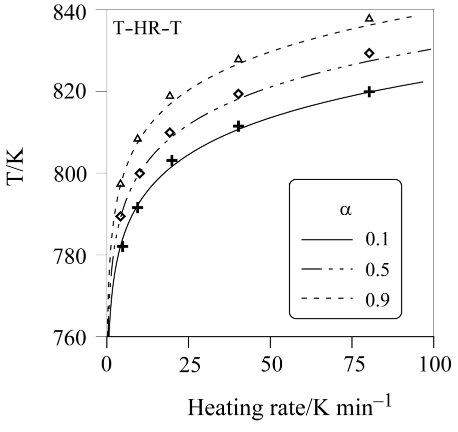

Fig. 2 Temperature–Heating Rate–Transformation diagram of the crystallization process of an Fe–Ni based metallic glass. Experimental data (symbols) and calculated curves (lines) for transformed fractions 0.1, 0.5 and 0.9

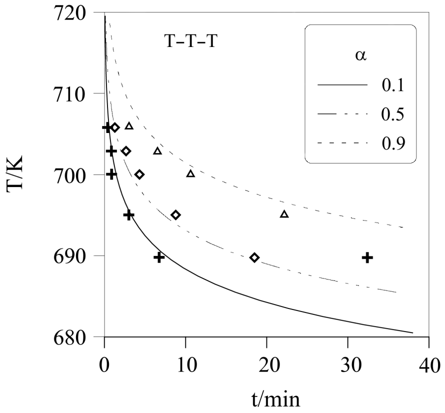

Fig. 3 Temperature–Time–Transformation diagram: Fe–Ni based metallic glass. Experimental data (symbols) and calculated curves (lines) for transformed fractions 0.1, 0.5 and 0.9

of material crystallized during treatment of the samples at a certain constant heating rate (temperature).

Solidification from the melt

The Arrhenius equation approach cannot be applied to solidification from the isotropic melt because this equation expresses a transformation rate increase as a function of temperature, while in solidification processes the rate behaves reversibly. The reason is that in this case the process is driven not by nucleus growth, but by nucleation. Hence, a certain amount of undercooling, $\Delta T=T_m-T$, is necessary to induce solidification [27]. The driving force for nucleation is the Gibbs energy difference (ΔG) between the liquid and the crystal. At low undercooling, $\Delta G\approx\Delta S_m\Delta T$, with ΔS_m the melting entropy [28]. However, an interfacial energy, σ, is necessary to form the interface between the liquid and the nucleus. As a consequence, the size of the fluctuating forming nucleus has to be larger than a critical size to be able of growth. Irrespective of the mode of growth, nucleation is activated by a crystallization rate constant, K, which is proportional to some power of the nucleation frequency. According to these assumptions the rate constant can be approximated to

$$K(T)=A\exp(-B/T(\Delta T)^2) \tag{8}$$

where A displays a smooth dependence on temperature with respect to the exponential factor, and B is a constant proportional to $\sigma^3/\Delta S_m^2$ [28].

Here, an isoconversional method, similar to the usually applied to find the activation energy for a given degree of conversion, transformed fraction, α, is developed to evaluate the constant B in the case of solidification from an isotropic melt. A description of the isoconversional method is given in [29, 30]. Calculation of constant B is based on a multiple-scan method that requires several measurements at different cooling rates. If we repeat the procedure for different values of α, the invariance of B with respect to α (which is a basic assumption for the validity of the model) is checked in a simple and reliable manner. This operation allows testing the melting temperature T_m accuracy at same time. A first estimation of T_m results from previous heating, where samples are completely melted.

Once B and T_m are known, it is possible to evaluate directly from the experimental data the kinetic model. Nevertheless, the knowledge of the kinetic model is not necessary to obtain the transformation diagrams. From the B and T_m values and using Eq. (8), the integral from Eq. (1) under isothermal regime at temperature T_0 up to a degree of crystallinity α_0 (annealing time t_0) *is*

$$g(\alpha)=\exp\,[-B/T_0(\Delta T_0)^2]t_0 \tag{9}$$

with $\Delta T_0=T_m-T_0$.

Similarly, under continuous cooling at a rate c, the integrated form of Eq. (1) under cooling conditions becomes

$$g(\alpha_0)=\int_0^{\Delta T}\exp(-B/T(\Delta T_0)^2)\frac{d(\Delta T_0)}{c} \tag{10}$$

The quantity $g(\alpha_0)$ is independent of the mode of crystallization, i.e. isothermal conditions or continuous cooling conditions. Once its value for a given transformed fraction α_0 is known, the analytical expression for $g(\alpha_0)=g(\alpha_0(T,t))$ for any pair (T,t) is given by

$$\exp\left(-\frac{B}{T(\Delta T_0)^2}\right)t_0=\exp\left(-\frac{B}{T(\Delta T_0)^2}\right)t \tag{11}$$

In this way, we can obtain the pairs (T,t) that produces the same transformed fraction.

The analytical expression of $g(\alpha_0)=g(\alpha_0(T,c))$ for any pair (T,c) is given by

$$\int_0^{\Delta T}\exp\left(-\frac{B}{T(\Delta T_0)^2}\right)\frac{d(\Delta T)}{c_0}=\int_0^{\Delta T}\exp\left(-\frac{B}{T(\Delta T)^2}\right)\frac{d(\Delta T)}{c} \tag{12}$$

We can obtain the pairs (T,c) producing the same transformed fraction. Thus, the forms of the curves $T=T(t)$ and $T=T(c)$ for a fixed value of α, are obtained by means of the previous equations. Figures 4, 5 and 6 show calculated T–CR–T and T–T–T curves (lines) and several experimental DSC data (symbols) for transformed fractions corresponding to 0.1, 0.5 and 0.9 for a pharmaceutical blend PEG–PD. As expected in any solidification process, the solidification onset shifts to higher temperatures when the cooling rate decreases. We can state that the model gives a good description of the solidification process.

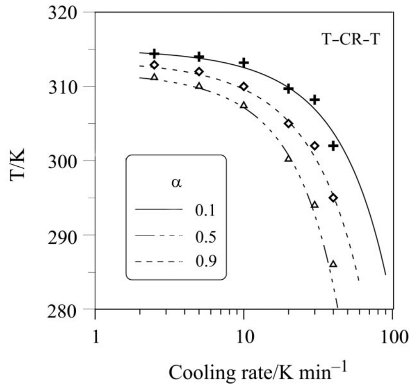

Fig. 4 Temperature–Cooling Rate–Transformation diagram of the solidification process of a pharmaceutical blend (PEG–PD). Experimental data (symbols) and calculated curves (lines) for transformed fractions 0.1, 0.5 and 0.9

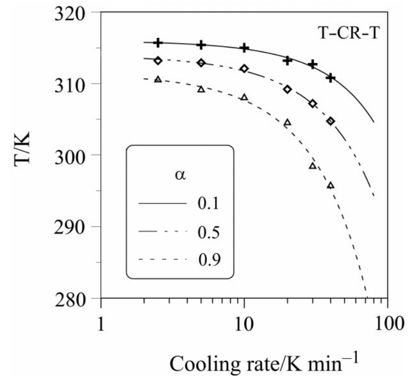

Fig. 5 Temperature–Cooling Rate–Transformation diagram of the solidification process of a pharmaceutical blend (PEG–PD). Experimental data (symbols) and calculated curves (lines) for transformed fractions 0.1, 0.5 and 0.9

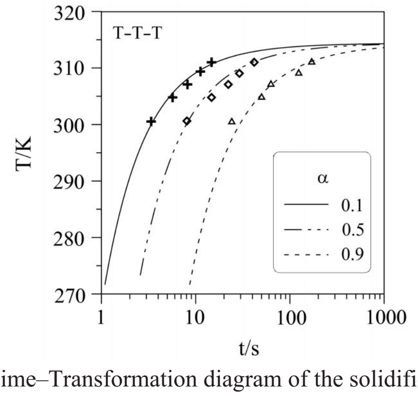

Fig. 6 Temperature–Time–Transformation diagram of the solidification process of a pharmaceutical blend (PEG–PD). Experimental data (symbols) and calculated curves (lines) for transformed fractions 0.1, 0.5 and 0.9

Conclusions

Transformation diagrams are one of the most reliable ways to predict the thermal behavior of the materials. Once a kinetic model has been determined, one can construct the transformation diagrams. However, in this work the diagrams were constructed without the knowledge of the kinetic model using calorimetry experiments. All the transformation curves are obtained from non-isothermal data. Two isoconversional methods are applied to perform the kinetic analysis. The methods were applied to analyze the cold crystallization and the solidification from the melt respectively.

The usefulness of the methods is illustrated by analysis of the crystallization process in two model materials: blends of polyethylene glycol 6000 with a pharmaceutical drug (PEG–PD) and Fe–Ni based metallic glasses obtained by rapid solidification (Fe–Ni). A good concordance is observed between the experimental curves obtained in the transformation diagrams by calculation and the experimental data, which verifies the reliability of the methods.

* * *

Financial support from CICYT (project MAT2000-0388) and DURSI (project SGR2001-00190) is acknowledged.

References

1 N. Clavaguera, J. Saurina, J. Lheritier, J. Masse, A. Chauvet and M. T. Mora, Thermochim. Acta, 290 (1997) 173.
2 W. A. Johnson and K. F. Mehl, Trans. Am. Inst. Min. Metall. Eng., 135 (1939) 416.
3 M. Avrami, J. Chem. Phys., 7 (1939) 103; 8 (1940) 212; 9 (1941) 177.
4 A. N. Kolmogorov, Izk. Akad. Nauk USSR, Ser. Mater., 3 (1937) 355.
5 D. R. Uhlmann. J. Non-Cryst. Solids, 7 (1972) 337.
6 J. J. Suñol, N. Clavaguera and M. T. Mora. J. Therm. Anal. Cal., 52 (1998) 853.
7 I. Yamauchi, T. Nagase and I. Ohnaka, J. Alloys and Comp., 202-1 (1999) 181.
8 I. Harismendy, C. M. Gómez, M. Delrio and I. Mondragón, Polymer Int., 49-7 (2000) 735.
9 A. J. Gavrin and E. P. Douglas, Macromolecules, 34-17 (2001) 5876.
10 S. Malinov, P. Markovsky, W. Sha and Z. Guo, J. Alloys and Comp., 314-1 (2001) 181.
11 H. Takebe, D. J. Brady, D. W. Hewak and K. Morinaga, J. Non-Cryst. Solids, 258 (1999) 239.
12 C. Y. Li, D. Yan, S. Z. D. Cheng, F. Bai, J. J. Ge, B. H. Calhoun, T. He, L.-C. Chien, F. W. Harris and B. Lotz, Phys. Rev. B, 60-18 (1999) 12675.
13 C. Basire, D. A. Ivanov, Phys. Rev. Letters, 85-26 (2000) 5587.
14 M. C. Weinberg, Thermochim. Acta, 194 (1992) 93.
15 F. Carrasco and P. Pagès, J. Appl. Pol. Sci., 61 (1996) 187.
16 S. Suriñach, M. D. Baró, J. A. Diego, N. Clavaguera and M. T. Clavaguera-Mora, Acta Metall. Mater., 40 (1992) 37.
17 M. T. Clavaguera-Mora, S. Suriñach, M. D. Baró and N. Clavaguera, J. Phys. D, 25 (1992) 803.
18 J. W. Christian, in 'Theory of Transformation in Metals and Alloys', Pergamon, Oxford 1975, Chap. 12.
19 N. Sbirrazzuoli, L. Vincent, J. Bouillard and L. Elégant, J. Therm. Anal. Cal., 56 (1999) 783.

20 P. Budrugeac, D. Homentcovschi and E. Segal, J. Therm. Anal. Cal., 63 (2001) 457.
21 P. Budrugeac, J. Therm. Anal. Cal., 68 (2002) 131.
22 J. M. Criado, J. Málek and A. Ortega, Thermochim. Acta, 147 (1989) 377.
23 J. Málek, Thermochim. Acta, 200 (1992) 257.
24 J. Málek, Thermochim. Acta, 267 (1995) 61.
25 S. Suriñach, M. D. Baró, M. T. Mora and N. Clavaguera, J. Non-Cryst. Solids, 58 (1983) 209.
26 S. Bordas, M. T. Mora and N. Clavaguera, J. Non-Cryst. Solids, 58 (1983) 209.
27 D. Turnbull, Contemp. Phys., 10 (1969) 473.
28 N. Clavaguera, J. Non-Cryst. Solids, 162 (1993) 40.
29 R. Berlanga, J. Farjas, J. Saurina and J. J. Suñol, J. Therm. Anal. Cal., 52 (1998) 765.
30 J. J. Suñol, In: 'Polymer Crystallization: new trends and applications', Springer (to be published).